THE JOURNAL OF PHYSICAL CHEMISTRY B

Article

pubs.acs.org/JPCB

# Poling Induced Mass Transport in Thin Polymer Films

Edgars Nitiss,[†] Eduards Titavs,[†] Karlis Kundzins,[†] Andrej Dementjev,[‡] Vidmantas Gulbinas,[‡] and Martins Rutkis*[,†]

[†]Institute of Solid State Physics, University of Latvia, Kengaraga street 8, Riga, Latvia

[‡]Lithuanian Center of for Physical Sciences and Technology, A. Gostauto street 11, Vilnius, Lithuania

**ABSTRACT:** In this study we report investigation of the polymer film morphology modifications during their corona poling for fabrication of nonlinear optically (NLO) active materials. We demonstrate that at certain poling conditions surface and spatial inhomogeneities in the poled area of the sample appear. Densities of the inhomogeinities depend on the strength of the poling field, the sample temperature during the poling, and the prepoling conditions. Optimization of the poling conditions directed toward avoiding surface modifications enables us to increase the overall observable effective nonlinearity of the sample up to 10 times. To investigate, understand, and eventually explain the formation of the spatial and surface structure inhomogeinites in the poled material we have used optical, second harmonic, and scanning electron microscope measurements, as well as the conductivity measurements of the thin films. We present results of poled polymer host−guest films where (dimethylamino)benzylidene-1,3-indandione and low dipole moment 2,2′,2″-(4,4′,4″-nitrilotribenzylidene)triindan-1,3-dione were used as guests in poly(methyl methacrylate), polystyrol, and polysulfone matrixes doped at 10 wt %.

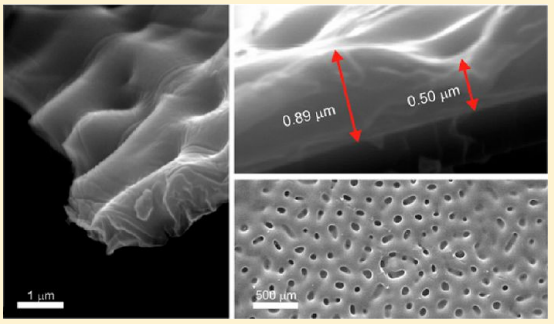


## INTRODUCTION

Nonlinear optically (NLO) active polymers doped with polar molecules are promising substitutes of NLO active inorganic materials for modern electronics. An increasing interest to new nonlinear optical (NLO) active organic materials is related to their low cost, easy processability, and potential applications as optical components in electro-optic (EO) modulators, optical switches, sensors, etc.[1,2] Such materials must possess large second-order nonlinear coefficients, which can be obtained by electric poling with corona discharge.[3−9] For maximal possible NLO efficiency one must achieve the highest polar order of dopant molecules in the system maintaining the chromophore structure, concentration, and optical properties of thin films. For polymer poling purposes the corona triode device is very attractive because one can have good control of the ion source and the poling field. The poling efficiency depends on multiple parameters such as poling temperature, electric field, etc. The corona poling possesses also several drawbacks. It takes a lot of effort for one to obtain controllable corona discharge and poling conditions due to the complexity of the discharge process. It has also been reported that poling with corona discharge may influence the surface quality of the film which is usually attributed to the bombardment of the film by accelerated ions.[10−12]

The second-order nonlinearity of poled material can be characterized using the second-order polarizability $\chi_{zzz}^{(2)}$

$$\chi_{zzz}^{(2)} = C\beta_{\mu}\langle\cos^3\vartheta\rangle \tag{1}$$

where $C$ is the chromophore concentration, $\beta_{\mu}$ is the molecular second-order polarizability projection on the dipole moment of molecule, and $\langle\cos^3\vartheta\rangle$ is the order parameter or the averaged cosine cube of angular difference between the dipole moment of the molecule and poling field.[13] The order parameter, according to an analytic approximation,[14] can be expressed as

$$\langle\cos^3\vartheta\rangle = \frac{\mu E}{5kT}\left[1 - L^2\left(\frac{W_{es}}{kT}\right)\right] \tag{2}$$

where $E$ is the poling field, $T$ is the poling temperature, $k$ is the Boltzmann constant, $\mu$ is the dipole moment of the molecule, $L$ is the Langevin function, and $W_{es}$ is the chromophore−chromophore electrostatic energy. The relation 2 may be divided into two parts. The first part, $\mu E/5kT$ describes the order parameter as a function of poling ($\mu E$) and the thermal depolarization ($kT$). As can be seen from (2), it is desirable to have the poling ($\mu E$) energy as high as possible for maximal ordering. This obviously can be achieved by increasing the poling field $E$ strength. However, surface irregularities may appear, as shown previously.[10−12] As a result, optical quality of the film is reduced and light scattering takes place. The second part of (2) ($1 - L^2(W_{es}/kT)$) expresses the dipole−dipole interactions in the material, which tend to reduce the order parameter due to repulsion of dipoles oriented in same direction. The dipole−dipole interactions could be also

**Received:** November 6, 2012
**Revised:** January 24, 2013
**Published:** February 12, 2013

responsible for the reduction of the NLO efficiency by stimulating formation of centrosymmetric NLO inactive aggregates, especially in guest–host systems where chromophores can move within a matrix.

In this contribution we present investigation of the spatial and surface irregularities in the guest–host polymer films poled at high field strength by the corona triode device. We have used a computer controlled corona triode device, which allows us to capture current–voltage characteristics of the system as well as to perform NLO polymer poling at constant grid potential or sample current. We show that similar changes in thin film morphology appear for all used host materials.

## EXPERIMENTAL SECTION

The investigated polymer host–guest films were prepared as follows. We used (dimethylamino)benzylidene-1,3-indandione (DMABI[15]) and low dipole moment 2,2′,2″-(4,4′,4″-nitrilotribenzylidene)triindan-1,3-dione (A3BI[16]) chromophores as guests in various matrixes (poly(methyl methacrylate) (PMMA, Sigma-Aldrich), polystyrene (PS, Sigma-Aldrich), and polysulfone (PSU, Sigma-Aldrich)) doped at 10 wt %. The films were spin-coated from a chloroform solution onto an ITO covered glass slide (SPI Supplies, ITO sheet resistivity 70–100 Ω). The glass transition temperatures of the samples were approximately 110 °C for the PMMA, 63 °C for the PS, and 119 °C for the PSU thin films. The thickness of the spin-coated samples was around 2 μm.

For sample poling we used a computer controlled corona triode device, which allows us to monitor and control the poling conditions. The principal scheme of corona triode setup[17] is shown in Figure 1. During the corona poling, high

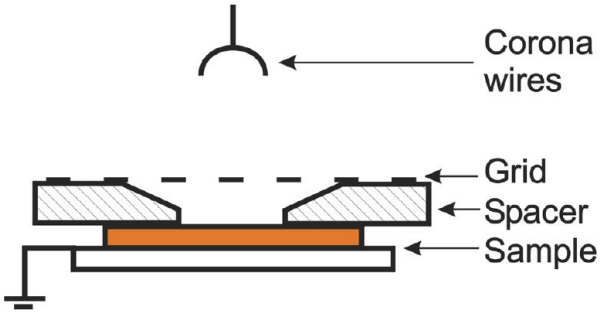


**Figure 1.** Principal scheme of corona discharge device.

voltage is applied to corona wires. By varying the grid voltage, we are able to control the polymer poling voltage. The voltage difference between corona wires and grid was kept constant of 9 kV to ensure invariable corona discharge conditions at different grid voltages. Ambient air in the corona chamber was replaced by nitrogen to keep the corona generated ionic composition and conductivity independent of temperature and moisture. The sample was put on the heater with precisely controlled temperature. We have also used spacers for varying the grid to sample distance. The spacer hollow has a conical shape; therefore, it acts as a lens for the ion flux allowing one to reduce the sample charging time at the beginning of the poling.

The resulting NLO efficiency and optical quality of the polymer films were found to depend on the poling procedure. One of the most common poling procedures includes turning on corona voltage after heating of the polymer to the glass transition temperature.[18,19] This procedure has an advantage of having polymer disposed of solvent and absorbed gases such as air and water vapor before chromophore orientation. However, at high guest concentrations many of chromophores tend to form aggregates and even crystals, which significantly reduce the NLO efficiency and the film quality. Turning on external electric field during the heating of the polymer film can prevent crystallization.[20] We used two poling procedures, which are schematically shown in Figure 2a,b. During the first poling

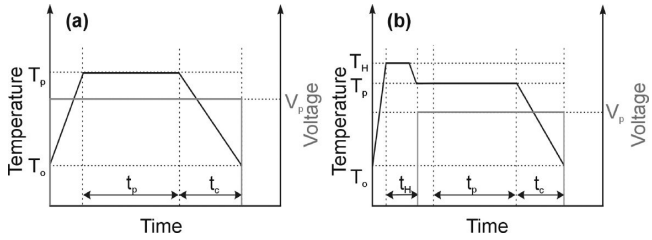


**Figure 2.** Time scale and parameters of (a) first corona poling procedure and (b) second poling procedure. $T_o$, $T_p$, and $T_H$ are the room, poling, and heating temperatures, respectively, $V_p$ is the poling/grid voltage, and $t_h$, $t_p$, and $t_c$ are the heating, poling, and cooling times, respectively.

procedure, as suggested by Vembris et al.,[20] the poling voltage was applied and kept constant while the sample was heated up to poling temperature $T_p$, poled and then cooled down to ambient temperature $T_o$. Such an approach reduced the amount of aggregates and crystals formed during the poling. However, we noticed that this poling procedure significantly increased probability of formation of spatial and surface inhomogeneities in the poled area of the sample. Therefore, we implemented the second poling procedure suggested by Lee et al.,[12] which allowed us to maintain good optical quality of poled thin films. It starts with a prepoling phase $t_H$ of approximately 3–5 min, during which the sample is heated to the preheating temperature $T_H$ with no poling field applied. The performed experiments show that this period of time is short enough to avoid formation of centrosymmetric crystals, but sufficiently long to dispose major part of the solvent and absorbed gases for the thin film. Afterward, the sample is poled like in the first poling procedure.

We used second harmonic generation (SHG) measurements with a setup[15] to evaluate the NLO efficiency of the poled polymers. From the SHG scan we are able to obtain the NLO efficiency profiles of the poled polymer. The SH intensity was then normalized to the SH intensity generated in quartz crystal. The obtained value is the effective nonlinear optical (NLO) coefficient $d_{eff}$.

Optical (bright field) microscope (Nikon ECLIPSE L150), scanning electron microscope (SEM) (Carl Zeiss EVO 50 XVP), and two photon excitation luminescence (TPEL) and SHG microscopes were used for investigation of irregularities in the poled polymer films.

Both TPEL and SHG images of poled polymer films were obtained through raster scanning of samples using a nonlinear optical scanning microscope. Excitation with picosecond pulses at 1064 nm wavelength and 1 MHz repetition rate was applied. An integral TPEL signal in a range from 540 to 710 nm was collected by using two cutoff filters (Thorlabs, Asahi-Spectra). The SHG signal was filtered with a laser line filter at 532 nm with the fwhm of 10 ± 2 nm (Thorlabs). The SHG imaging was performed at two perpendicular polarizations.


dx.doi.org/10.1021/jp310961a | J. Phys. Chem. B 2013, 117, 2812–2819

## RESULTS

Sample corona poling by the first procedure at certain poling conditions caused appearance of optical inhomogeneities in the poled part of the film. The optical inhomogeinities were caused by surface and/or spatial irregularities. As the size of inhomogeneities is close to the optical wavelength, light scattering takes place, and the poled area looks frosted. Optical microscope images of the unpoled region of PMMA+DMABI 10 wt % thin films and poled by the first poling procedure are shown in Figure 3a,b.

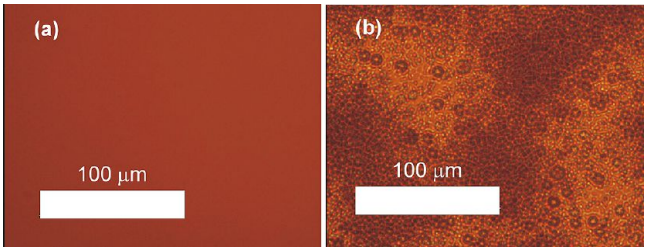


**Figure 3.** Optical images of the unpoled (a) and poled (b) regions of PMMA+DMABI (10 wt %) thin film obtained by the first poling procedure.

As mentioned before, higher NLO efficiencies should be obtained by increasing the poling field strength. However, as the poling field strength increases, the overall observable NLO efficiency drops down. This can be seen in Figure 4 where the

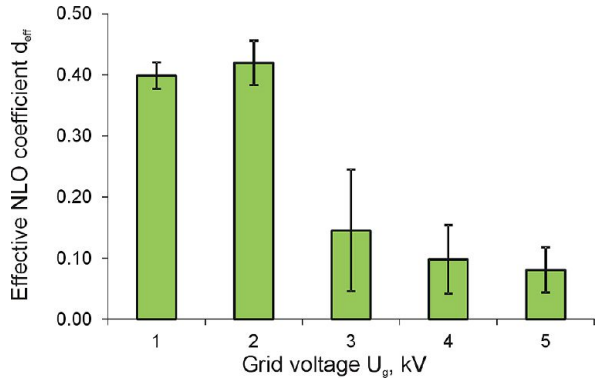


**Figure 4.** Effective NLO coefficient $d_{eff}$ of PMMA+DMABI (10 wt %) thin films as a function of grid voltage for the samples poled by the first poling procedure.

effective NLO coefficient $d_{eff}$ as a function of the grid voltage is shown. Clearly modification of the morphology of the poled area plays a significant role for the overall observable NLO efficiency. According to our observations, the inhomogeinities appear for all of the used hosts (PMMA, PS, and PSU). In Figure 5 optical images of poled areas of PMMA+DMABI (10 wt %), PS+DMABI (10 wt %), and (c) PSU+DMABI (10 wt %) thin films are shown.

The extent of the inhomogeneity was characterized by measuring the scattered light intensity. We found that the scattered light intensity depends on the poling electric field strength and the poling temperature, or simply on the ratio of poling and thermal energies. Figure 6 shows the scattered light

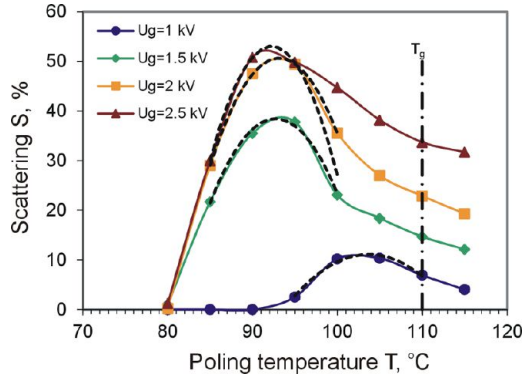


**Figure 6.** Scattered light percentage as a function of poling temperature at different grid voltages for PMMA+DMABI (10 wt %) thin films.

intensity as a function of poling temperature at different grid voltages. The light scattering from the poled part of the sample appears above the poling temperature of 80 °C. The scattered light intensity reaches maximum for sample poled at about 90 °C and then decreases as the poling temperature increases. The decrease is most probably caused by the reduction of amount of scattering elements due to decrease in viscosity, which favors the film fluidity and thus, reduction of film damage or some kind of "self-curing" takes place. The maximum of the scattered light intensity appears when higher grid voltages are applied at lower poling temperatures.

Figure 7 shows the poling temperatures at which the maximal scattered light intensity was obtained as a function of poling voltages. These values were obtained from the data displayed in Figure 6, where the points around the maximal scattering value are approximated by a second-order polynomial function. After the temperatures at which maximal light scattering takes place are identified, they are displayed as black points in Figure 7. The black point approximation suggests that the product of poling temperature at which maximum scattering is obtained

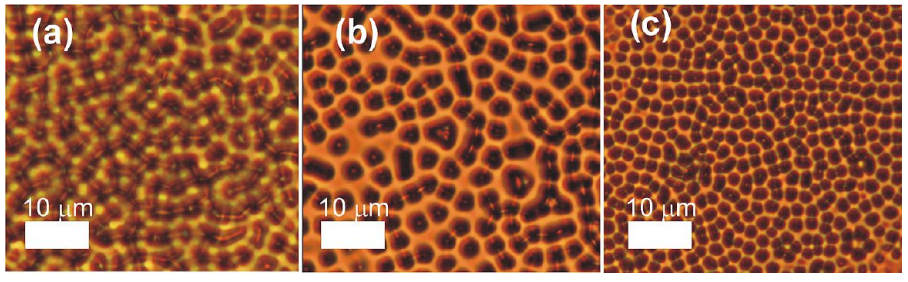


**Figure 5.** Optical images of the poled regions (a) PMMA+DMABI (10 wt %), (b) PS+DMABI (10 wt %), and (c) PSU+DMABI (10 wt %) poled applying first poling procedure.


dx.doi.org/10.1021/jp310961a | J. Phys. Chem. B 2013, 117, 2812−2819

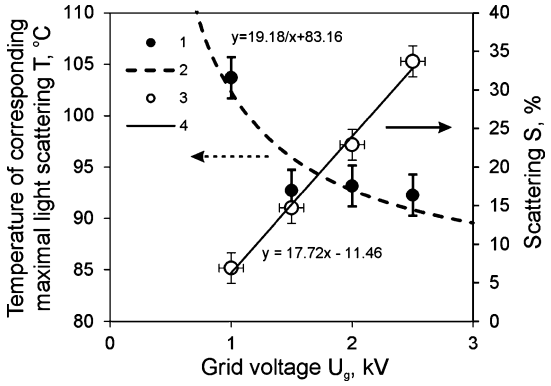


**Figure 7.** Temperature of corresponding maximal scattering as a function of poling temperature (1) and fit (2), scattering as a function of grid voltage for samples poled at $T_g$ = 110 °C (3), and linear fit (4) for PMMA+DMABI (10 wt %) thin films.

and the respective grid voltage at which poling is performed is constant or simply $T{\cdot}E$ = const. The temperature and grid voltage relation clearly attributes to the amount of energy necessary for the formation of scattering structure in the PMMA+DMABI (10 wt %) thin films. Figure 7 also shows the scattering intensity as a function of grid voltage for the samples poled at glass transition temperature $T_g$ = 110 °C. The scattering intensity in this case is directly proportional to the grid voltage value. Extrapolation of the linear dependence of scattering intensity to zero value gives that approximately 650 V is necessary for the surface irregularities to appear if the guest–host film is poled at glass transition temperature $T_g$.

Formation of the scattering structure depends also on the distance between the sample and the grid. Increase of the grid to sample distance reduces the ion energy and also weakens formation of the scattering structure. Figure 8 shows that the scattering intensity approximately linearly decreases with increase in the grid to sample distance.

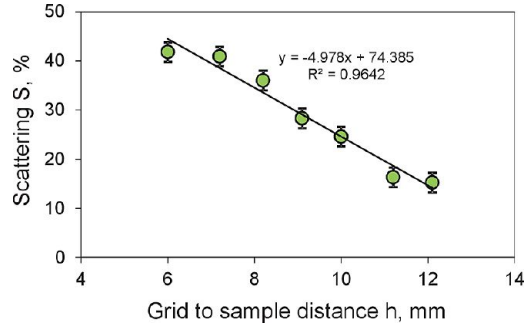


**Figure 8.** Scattered light percentage as a function of grid to sample distance for sample poled by the first poling procedure at constant grid voltage $U_g$ = 1.5 kV and poling temperature 95 °C.

Figure 9 shows the SEM image of the poled PMMA+DMABI (10 wt %) film. It reveals the "hilly" structure of the film surface, with the typical "hill" to "hollow" height differences of about 0.4 $\mu$m, i.e., close to the half of the film thickness. Parts a–d of Figure 10 show optical, SHG, and two photon excitation luminescence (TPEL) images of the poled sample area. As a first approximation, we assume that locally the TPEL signal is proportional to the concentration of chromophores, but the SH intensity characterizes the amount of noncentrosymmetric elements. Parts a–d of Figure 10 show that dark spots in optical images are also dark in the TPEL images, again suggesting that the dark spots are hollows meaning that the mass is dragged away from the center of the hollow during the poling. It shall be also noticed that there is an increased TPEL and SH signal around the hollows.

From the analysis of the SH images, we see that only the hollow slopes are NLO active as is shown in Figure 11a,b at orthogonal excitation light polarizations. Such pattern in SHG image is typical for radial arrangement of the nonlinear dipoles. Because the SH intensity characterizes the amount of noncentrosymmetric elements, the pattern in SHG image suggests that the chromophores (dipoles) are oriented toward or away from the hollow centers.

The thin films maintain their optical quality if they are poled by the second poling procedure described above. When we compare NLO efficiencies at the centers of the samples poled at the same temperature and grid voltage, we find the samples poled by the second poling procedure show at least 6 times higher efficiency compared to the ones poled by first poling procedure. The effective NLO coefficients $d_{eff}$ are shown in Figure 12. One would expect higher NLO activity from material poled by the first poling procedure than from material poled by the second procedure, due to the fact that fewer molecules are expected to form aggregates and crystals during the heating phase.[9] However, as the light scattering in the poled area takes place, the overall observable effective NLO activity of material is reduced. We also measured the NLO efficiency of the poled thin films as a function of grid voltage. From the experimental data shown in Figure 4 it can be seen that for the sample poled by the first poling the NLO efficiency decreases by increasing the grid voltage, on the contrary the NLO efficiency increases with the grid voltage as shown in Figure 13a if the second poling procedure was applied.

Because the effective NLO coefficient of the poled thin film depends on the electric field, we investigated also how the effective poling voltage depends on the grid to sample distance. In Figure 13b the effective NLO coefficient $d_{eff}$ as a function of grid to sample distance for the films poled by second poling procedure at grid voltage 1.5 kV is shown indicating no clear dependence. This means that the sample was charged to a certain voltage (not higher than the grid voltage) regardless of the sample to grid distance.

We have analyzed surfaces of the PMMA+DMABI (10 wt %) samples how they depend on the prepoling and poling temperatures (Figure 14). For the characterization of the sample surfaces we used two possible states. Filled circles in Figure 14 mark the samples, which have changed their surface morphology, and empty circles represent the samples that have maintained their optical properties after the poling. All the samples were poled using the second poling procedure at 2.5 kV grid voltage. The dotted lines mark the glass transition temperature. On the basis of these results, we were able to determine the boundary at which in case second poling procedure is used the samples change their surface morphology. This boundary is indicated as a line dividing gray and white regions in the graph (Figure 14). If the prepoling and poling temperature values are chosen with coordinates ($T_{pp}$, $T_p$) that correspond to a point in the gray (white) region in Figure 14, the surface inhomogeinities will (will not) appear during the poling. It should also be noted that if samples are poled above glass transition temperature, there will always be changes in the sample surface morphology. To get the highest possible nonlinearity of the thin film, one should pole the samples


dx.doi.org/10.1021/jp310961a | J. Phys. Chem. B 2013, 117, 2812–2819

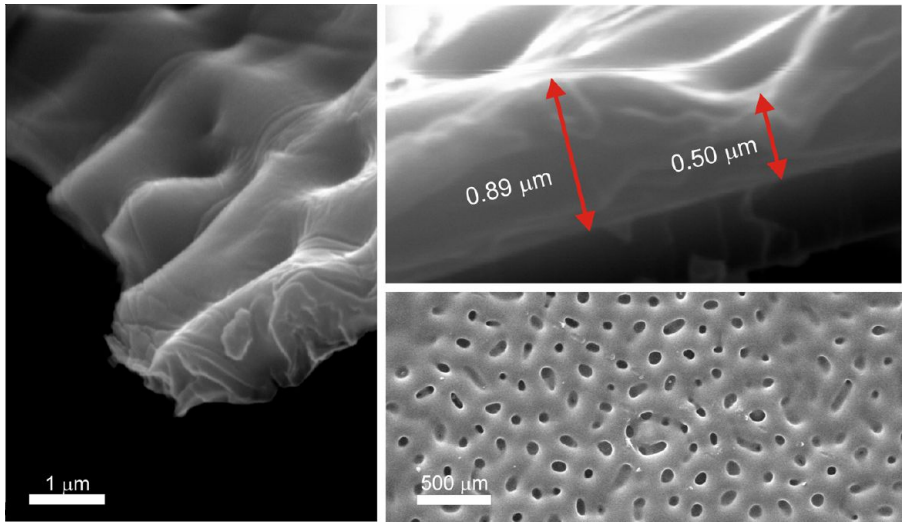


**Figure 9.** Electron microscope image of poled part of PMMA+DMABI (10 wt %) thin film.

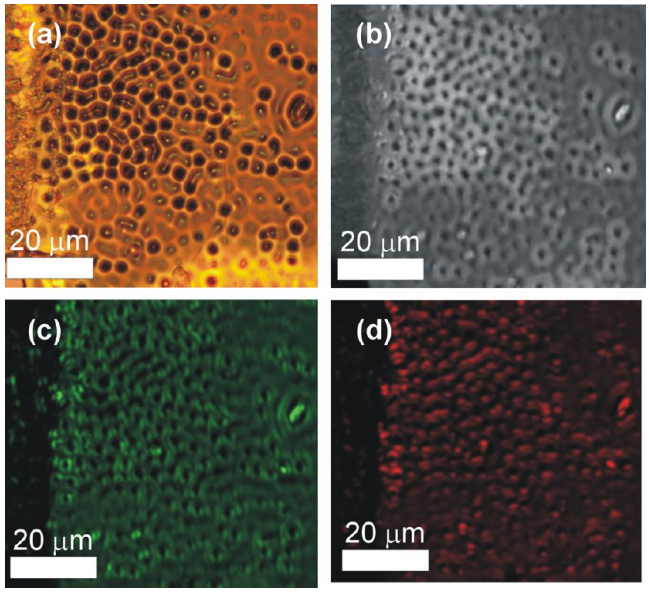


**Figure 10.** (a) Optical image, (b)TPEL, (c) SHG horizontally polarized (0°) and (d) SHG vertically polarized (90°) images of poled area of PMMA+DMABI (10 wt %) thin film.

using second poling procedure with prepoling and poling temperatures corresponding to a point that is as close as possible to the intersection of the glass transition temperature lines, but below the gray–white region boundary line. In this particular case for PMMA+DMABI (10 wt %) sample the poling temperature should be 105 °C and the prepoling temperature 115 °C.

Because the conductivity of the thin film could also influence the formation of surface irregularities, we investigated whether there are differences in the conductivity of the nonpreheated and preheated samples. For these measurements a 100 nm thick Al electrode was sputtered on the thin films and $I-V$ characteristics were captured. The results are shown in Figure 15. It can be clearly seen that the current at respective voltages is lower for the preheated samples.

## DISCUSSION

As shown above, formation of the film inhomogenieties depend on the poling and prepoling procedures. There could be three main reasons for the formation of inhomogenieties in the guest host films during the poling. First, we suggest that the hollows are formed by the charged ions, which ram the soft polymer. The speed and therefore kinetic energy of ions depend on the grid potential and on the grid to sample distance. A second hypothesis would be that the hollows are formed due to mass transport induced by the poling field and chromophore dipole interaction. Numerical Langevin dynamics calculations imply that molecules, if not bound, due to dipole–dipole interactions can move, forming high-order structures during the poling procedure,[21] or in other words, mass transport can take place. In such a way chromophores, while creating polar elements, could drag the surrounding polymer. Finally, we would like to propose that the hollows could be made by local electrical breakdown of the polymer.

In the first two cases, polymer must be sufficiently soft for the changes in the morphology of the film to take place. Therefore, polymers must be poled at temperature higher than some critical value (Figure 6) for the inhomogeinities to appear. Unfortunately, both the formation of hollows due to high energy ion bombardment and the dipole moment–electric field interaction induced mass transport depend on the polymer poling temperature and poling field. This fact causes the difficulties to favor either of these two hypotheses on formation of surface inhomogeinities.

There are facts that would favor either the first or the second hypothesis of the formation of surface inhomogeinities. From Figure 8 it is obvious that the density of scattering elements grows if the grid is closer to the sample. This clearly favors the hypothesis that the hollows are formed during the ion impact. Increasing the grid to sample distance (assuming that the free path length does not change) we increase the probability for the charged ion to lose part of its kinetic energy during impacts in the space between grid and sample. Therefore, at the same initial potential energy conditions determined by the grid voltage, at higher sample to grid distances, the ions will have less kinetic energy left to transfer to the polymer film. Because the thin film poling voltages do not depend on the sample to grid distance (Figure 13b), the magnitude of poling field and


dx.doi.org/10.1021/jp310961a | J. Phys. Chem. B 2013, 117, 2812–2819

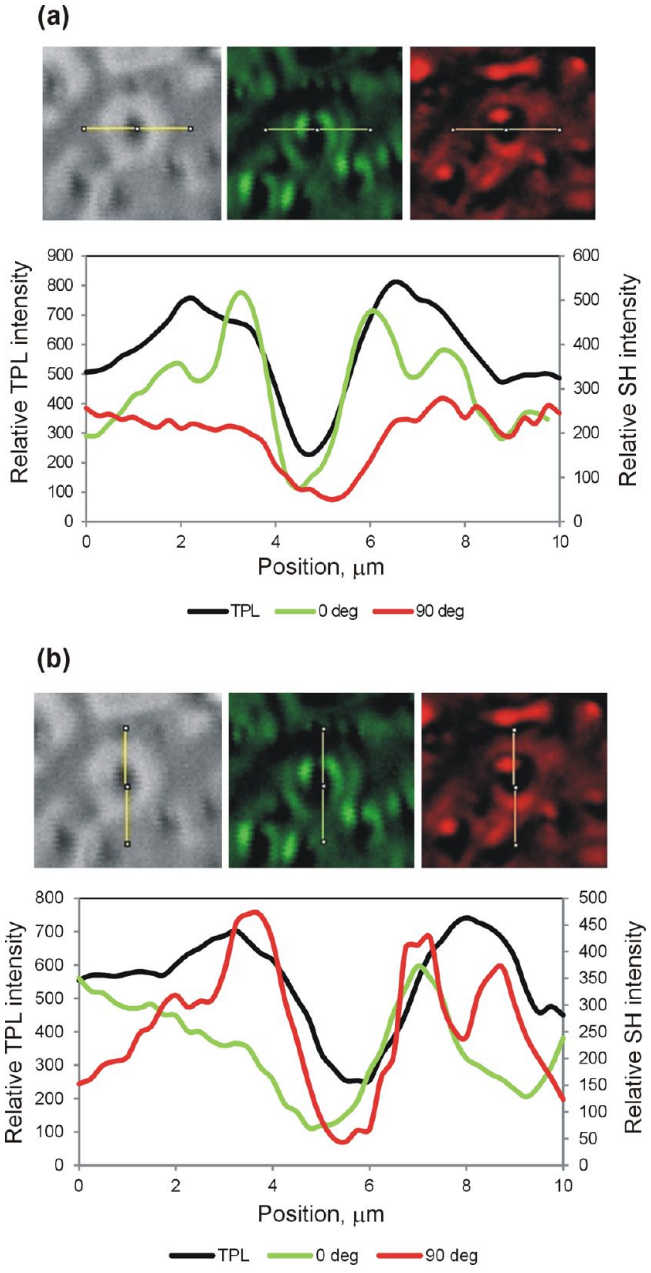


**Figure 11.** Caption TPEL and SHG intensities of the hollows scanned (a) vertically and (b) horizontally after excited by horizontally polarized (0°) and vertically polarized (90°) light.

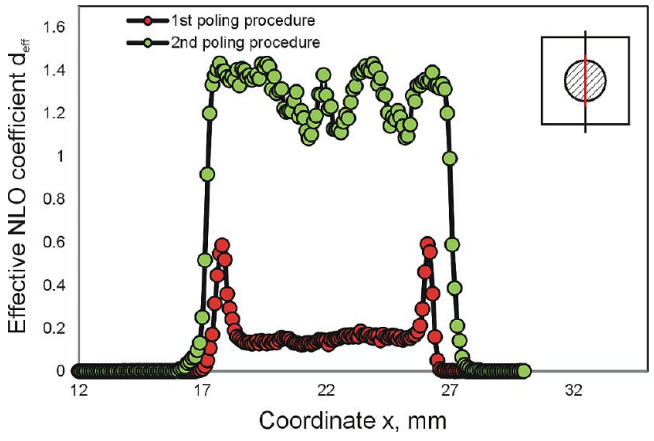


**Figure 12.** SHG scan: effective NLO coefficient $d_{eff}$ of PMMA +DMABI (10 wt %) thin films poled of using first and second procedure.

molecule dipole moment interaction also would not change. This again favors the fact that hollows are formed during the ion impact. As mentioned previously, to eliminate the chromophore and electric field interaction effect on the formation of hollows, samples with nonpolar A3BI chromophores were made and poled. We were not able to observe any changes in the sample morphology. This clearly suggests that the chromophores in guest–host films must possess a dipole moment so that the changes in thin film morphology would take place. The result favors the second hypothesis that the hollows are formed due to mass transport induced by the poling field and chromophore dipole moment interaction. The probability of hollow formation due to mechanical impact and poling field and chromophore dipole moment interaction is also influenced by the poling temperature, which defines the viscosity of the polymer. Partial reduction of inhomogeinities at higher poling temperatures suggests that polymer is sufficiently soft (fluent) for the hollows to close.

The reason why there are no inhomogeinities in the sample to which prepoling procedure is applied could be the following. After sample preparation, the films still contain some amount of solvent, so the ambient gases and water accumulate in polymer pores. Heating the sample causes the solvent and absorbed gases to leave the pores, thus increasing the polymer glass transition temperature.[22]

Therefore, after the preheating of the film, the glass transition temperature of polymer increases making the mass transfer less probable. We also performed hardness measurements for the thin PMMA+DMABI (10 wt %) films, which showed that the hardness of the thin film to which prepoling procedure was applied increased only by 18%. Such a small increase in hardness could not be the reason for such a dramatic change in the surface irregularity concentration. Because after the spin coating the molecules are frozen not in the energetically most favorable condition from the molecular interaction point of view, we suppose that the prepoling procedure enhances the relaxation processes in the film. Thus, after the prepoling procedure, the molecules have compacted, therefore reducing the probability of poling induced mass transport.

Finally, we found that conductivity of the preheated samples is lower than for the samples poled by the first poling procedure (Figure 15). This finding leads to our third hypothesis for the formation of surface irregularities. We propose that the hollows could be made by local electrical breakdown of the polymer. Because the samples poled by the first poling procedure have higher conductivities than the ones poled by the second poling procedure, it is more likely that local electrical breakdown will take place during the first poling procedure. At temperatures beyond glass transition temperature $T_g$, the solvent and absorbed gases have left the sample. This means that at temperature beyond the $T_g$ the conductivity would not depend on the prepoling procedure used. Because the conductivity of the polymer grows rapidly around $T_g$, the probability of electrical breakdown is a lot higher for samples poled at temperatures higher than $T_g$. This explains why the irregularities appear for both poling procedures at high enough poling temperatures.


dx.doi.org/10.1021/jp310961a | J. Phys. Chem. B 2013, 117, 2812–2819

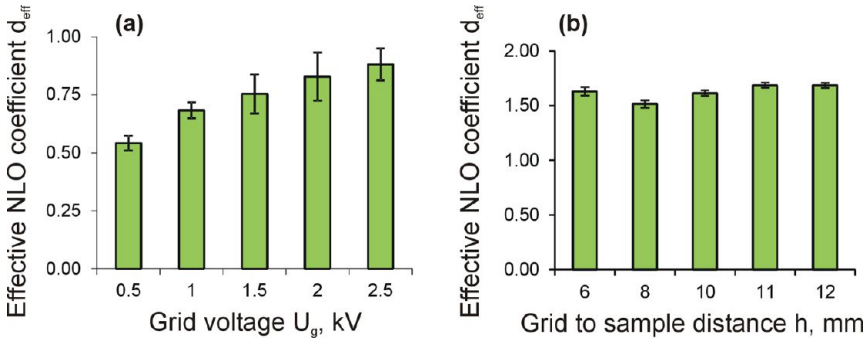


**Figure 13.** Caption effective NLO coefficient $d_{eff}$ of PMMA+DMABI (10 wt %) thin films as a function of (a) grid voltage for the samples poled by the second poling procedure and (b) sample to grid distance for the samples poled by the second poling procedure at $U_g$ = 1.5 kV.

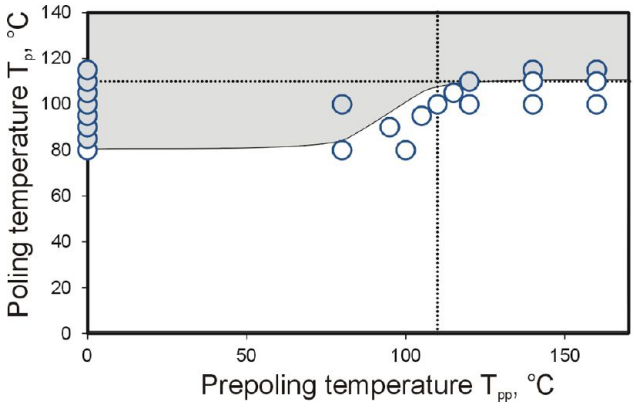


**Figure 14.** "Inhomogeneity" chart: surface condition at respective prepoling $T_{pp}$ and poling $T_p$ temperatures using the second poling procedure. The filled circles represent the samples, which have changed their surface morphology, and the empty circles represent the samples that maintained their optical properties. Black dotted lines represent the coordinates of the glass transition temperature.

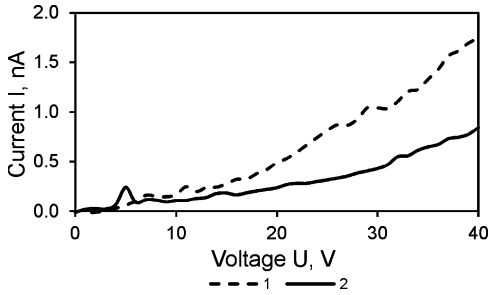


**Figure 15.** Current–voltage ($I$–$V$) characteristics of (1) nonpreheated and (2) preheated sample.

## CONCLUSIONS

In conclusion, we have investigated morphology changes of thin host–guest polymer films caused by corona poling procedure. Formation of surface irregularities was observed by reaching threshold poling temperatures at high poling fields for all used host polymers. The appearance of irregularities may be controlled by prepoling and poling conditions. A certain prepoling procedure helps to avoid formation of irregularities. It involves the film heating to temperatures higher than the poling temperature for a short period of time with no poling field applied. This approach helps to suppress formation of inhmogeinities for PMMA, PS, and PSU thin films doped with DMABI and increases the effective NLO efficiency. We also demonstrate that greater grid to sample distances additionally help to avoid irregularities, while keeping the poling efficiency unaffected.

We propose three hypotheses that could explain the effect of surface and morphology changes in the sample during the corona poling. The inhomogenieties in the form of hollows could be formed due to high energy ion bombardment. We have shown that the density of scattering elements or hollows grows if we increase the kinetic energy of the ions, which can be done either by increasing grid voltage or by decreasing the distance between the grid and sample surface. However, we were not able to observe any changes in the sample morphology when nonpolar chromophores are dissolved in the host. This suggests that polar molecules are required in the thin film to observe formation of inhomogenieties. Thus possibly the changes in the sample morphology are induced by the poling field and chromophore dipole moment interaction, which causes mass transport to take place. The mentioned hollows could also be formed by local electrical breakdown in the film. This hypothesis is encouraged by the fact that we were able to observe a correlation between the sample conductivity and probability for the changes in sample morphology to take place during the poling. Unfortunately, the mechanism of formation of these inhomogeneities is still unclear.

## AUTHOR INFORMATION

### Corresponding Author

*E-mail: martins.rutkis@cfi.lu.lv.

### Notes

The authors declare no competing financial interest.

## ACKNOWLEDGMENTS

This work has been supported by ERDF project (agreement No. 2010/0308/2DP/2.1.1.1.0/10/APIA/VIAA/051) and by the European Social Fund within the project "Support for Doctoral Studies at University of Latvia". We also acknowledge Roberts Zabels at the Institute of Solid State Physics for the polymer hardness measurements.

## REFERENCES

(1) Dalton, L. R. Rational Design of Organic Electro-Optic Materials. *J. Phys.: Condens. Matter* **2003**, *15*, 897–934.

(2) Cho, M. J.; Choi, D. H.; Sullivan, P. A.; Akelaitis, A. J. P.; Dalton, L. R. Recent Progress in Second-Order Nonlinear Optical Polymers. *Prog. Polym. Sci.* **2008**, *33*, 1013–1058.

(3) Hou, A.; Zhang, D.; Chen, K.; Yi, M. Poling of Organic Polymer Films for External Electro-Optic Measurement. *Proc. SPIE* **2000**, *3943*, 299–305.

(4) Marshall, J. M.; Zhang, Q.; Whatmore, R. W. Corona Poling of Highly (001)/(100)-Oriented Lead Zirconate Titanate Thin Films. *Thin Solid Films* **2008**, *516*, 4679−4684.
(5) Mönckе, D.; Mountrichas, G.; Pispas, S.; Kamitsos, E. I.; Rodriguez, V. SHG and Orientation Phenomena in Chromophore DR1-Containing Polymer Films. *Photonics and Nanostructures − Fundamentals and Applications* **2011**, *9*, 119−124.
(6) Yun, B.; Hui, G.; Lu, C.; Cui, Y. Study on Dipolar Orientation and Relaxation Characteristics of Guest-Host Polymers Affected by Corona Poling Parameters. *Opt. Commun.* **2009**, *282*, 1793−1797.
(7) Giacometti, J. A.; Fedosov, S.; Costa, M. M. Corona Charging of Polymers: Recent Advances on Constant Current Charging. *Braz. J. Phys.* **1999**, *29*, 269−279.
(8) Fukuda, T.; Matsuda, H.; Someno, H.; Kato, M.; Nakanishi, H. An Effective Poling of High Tg NLO Polymers. *Mol. Cryst. Liq. Cryst.* **1998**, *315*, 105−110.
(9) Vembris, A.; Rutkis, M.; Laizane, E. Influence Of Corona Poling Procedures on Linear and Non-Linear Optical Properties of Polymer Materials Containing Indandione Derivatives as Cromophores. *SPIE Proceedings, Organic Optoelectronics and Photonics III* **2008**, *6999*, 699924.
(10) Min, Y. H.; Lee, K.-S.; Yoon, C. S.; Do, L. M. Surface Morphology Study of Corona-Poled Thin Films Derived From Sol-Gel Processed Organic-Inorganic Hybrid Materials for Photonics Application. *J. Mater. Chem.* **1998**, *8* (5), 1225−1232.
(11) Hill, R. A.; Knoesen, A.; Mortazavi, M. A. Corona Poling of Nonlinear Polymer Thin Films for Electro-Optic Modulators. *Appl. Phys. Lett.* **1994**, *65*, 1733−1735.
(12) Lee, S.-S.; Garner, S. M.; Chuyanov, V.; Zhang, H.; Steier, W. H.; Wang, F.; Dalton, L. R.; Udupa, A. H.; Fetterman, H. R. Optical Intensity Modulator Based on a Novel Electrooptic Polymer Incorporating a High $\mu\beta$ Chromophore. *IEEE J. Quantum Electron.* **2000**, *36* (5), 527−532.
(13) Burland, D. M.; Miller, R. D.; Walsh, C. A. Second-Order Nonlinear Optical Active Calix[4]arene Polyimides Suitable for Frequency Doubling in the UV Region. *Chem. Rev.* **1994**, *94*, 31−75.
(14) Dalton, L. R.; Harper, A. W.; Robinson, B. H. The Role of London Forces in Defining Nocentrosymmetric Order of High Dipole Moment-High Hyperpolarizability Chromophores in Electrically Poled Polymeric Thin Films. *Proc. Natl. Acad. Sci. U. S. A.* **1997**, *94*, 4842−4847.
(15) Rutkis, M.; Vembris, A.; Zauls, V.; Tokmakovs, A.; Fonavs, E.; Jurgis, A.; Kampars, V. Novel Second-Order Non-Linear Optical Polymer Materials Containing Indandione Derivatives as Chromophores. *Proc. SPIE* **2006**, *6192*, 61922Q.
(16) Mihailovs, I.; Kreicberga, J.; Kampars, V.; Miasojedovas, S.; Jursenas, S.; Skuja, L.; Rutkis, M. Hyper-Rayleigh Scattering and Two-Photon Luminiscence of Phenylamine-Indandione Chromophores. *IOP Conf. Series: Mater. Sci. Eng.* **2012**, *38*, 012035.
(17) Vilitis, O.; Titavs, E.; Nitiss, E.; Rutkis, M. Chromophore poling in thin films of organic glasses. 3. Corona triode discharge setup. *Latv. J. Phys. Tech. Sci.* **2013**, *1*, 66−75.
(18) Mortazavi, M. A.; Knoesen, A.; Kowel, S. T. Second Harmonic Generation and Absorption Studies of Polymer-Dye Films Oriented by Corona-Onset Poling at Elevated Temperatures. *J. Opt. Soc. Am. B* **1989**, *6* (4), 733−741.
(19) Dao, P. T.; Williams, D. J.; McKenna, W. P.; Berarducci, K. G. Constant Current Corona Charging as a Technique for Poling Organic Nonlinear Optical Thin Films and the Effect of Ambient Gas. *J. Appl. Phys.* **1993**, *73*, 2043−2050.
(20) Vembris, A.; Rutkis, M.; Laizane, E. Effect of Corona Poling and Thermo Cycling Sequence on NLO Properties of the Guest-Host System. *Mol. Cryst. Liq. Cryst.* **2008**, *485*, 873−880.
(21) Rutkis, M.; Jurgis, A. Insight in NLO Polymer Material Behavior from Langevin Dynamic Modeling of Chromophore Poling. *Integr. Ferroelectr.* **2011**, *123*, 53−65.
(22) Wissinger, R. G.; Paulaiti, M. E. Glass Transitions in Polymer/CO2Mixtures at Elevated Temperatures. *J. Polym. Sci. Part B: Polym. Phys.* **1991**, *29* (5), 631−633.